

Title	Chained Turbo Equalization for Multiuser SIMO-OFDM Systems without Cyclic Prefix
Author(s)	Irawan, Ade; Anwar, Khoirul; Matsumoto, Tad
Citation	2012 International ITG Workshop on Smart Antennas (WSA): 301-306
Issue Date	2012-03-08
Type	Conference Paper
Text version	author
URL	<a href="http://hdl.handle.net/10119/10530">http://hdl.handle.net/10119/10530</a>
Rights	This is the author's version of the work. Copyright (C) 2012 IEEE. 2012 International ITG Workshop on Smart Antennas (WSA), 2012, 301-306. Personal use of this material is permitted. Permission from IEEE must be obtained for all other uses, in any current or future media, including reprinting/republishing this material for advertising or promotional purposes, creating new collective works, for resale or redistribution to servers or lists, or reuse of any copyrighted component of this work in other works.
Description	



# Chained Turbo Equalization for Multiuser SIMO-OFDM Systems without Cyclic Prefix

Ade Irawan\*, Khoirul Anwar\* and Tad Matsumoto\*<sup>§</sup>

\*School of Information Science

Japan Advanced Institute of Science and Technology (JAIST), 1-1 Asahidai, Ishikawa 923-1292, JAPAN

Email: {ade.irawan, anwar-k, matumoto}@jaist.ac.jp

<sup>§</sup>Center for Wireless Communications, University of Oulu, Finland

Email: tadashi.matsumoto@ee.oulu.fi

**Abstract**—Chained turbo equalization (CHATUE) is a simple detection scheme for block transmission without cyclic prefix (CP), where turbo equalizers for the several consecutive frames exchange information about the interference components in the form of a *a posteriori* Log-Likelihood Ratio (LLR). Although elimination of CP in the block transmission can significantly increase bandwidth efficiency, the received signal suffers from inter-block interference (IBI), which can not be effectively compensated by block-by-block equalization.

In this paper, we apply the CHATUE algorithm to effectively suppress inter-symbol interference (ISI), inter-carrier interference (ICI), and multiple-access interference (MAI) in a Multiuser Single Input Multiple Output Orthogonal Frequency Division Multiplexing (MU-SIMO-OFDM) system without CP. Results of computer simulations show the superiority of our proposed MU-SIMO-OFDM to conventional CP-aided systems, without requiring high computational complexity. The convergence property of the proposed technique is analyzed using the extrinsic information transfer (EXIT) chart. Doped accumulator is used to achieve a mutual information point close enough to the (1,1) point, and also to obtain better matching between the equalizer and decoder EXIT curves.

## I. INTRODUCTION

Orthogonal frequency division multiplexing (OFDM) has been chosen for several wireless broadband standards such as IEEE 802.16 wireless metropolitan networks, IEEE 802.11a and HIPERLAN/2 wireless local area networks, terrestrial digital audio broadcasting (DAB-T), and terrestrial video broadcasting (DVB-T). Such services need to accommodate as many users as possible within the limited frequency bandwidth. Therefore, spectrally efficient broadband schemes have to be created. Multiple input multiple output (MIMO) techniques provide answers without requiring additional bandwidth to this problem in the form of spatial multiplexing. Hence, A combination of MIMO and OFDM appears to be one of the most efficient techniques for next generation broadband wireless systems.

In OFDM systems, the guard interval such as cyclic prefix (CP) is used to avoid the inter-symbol interference (ISI). The CP-aided transmission converts the block-wise channel matrix structure from Toeplitz to circulant, which can significantly reduce the computational complexity of the detection schemes. However CP insertion imposes loss in bandwidth efficiency. In order to cope with this problem and enhance the spectrum

efficiency, OFDM systems, with insufficient or even no CP-aided transmission have been presented in literatures [4][5]. Equalization both in the time domain and in the frequency domain of single input multiple output OFDM (SIMO-OFDM) systems with insufficient CP has been investigated in [3]. In the time domain process, a block linear equalizer is applied on the  $r$ th receive antenna. The equalizer is designed based on maximizing the signal-to-interference-plus-noise ratio (SINR). The computational complexity due to the matrix inversion can be reduced using a low-rank approximation, as introduced in [8], as a part of the channel estimation process. Meanwhile, in frequency domain process, the equalization is carried out by sliding fast Fourier transforms (FFT) operation per  $n$ -tone of subcarriers. In order to reduce the computational complexity, the authors applied the technique which was introduced in [2].

Equalization technique for SIMO-OFDM systems without CP-transmission by using ISI-free transformation has been presented in [9]. It is simply by performing multiplication of the received signal with the orthogonal complement of the interference-component matrix, followed by filtering. Therefore, interferences removal can be achieved. However, the multiplication ruins the orthogonality of the channel matrix, thereby increases the inter-carrier interference (ICI). To solve this problem, ICI-free filter is used to reduce the ICI effect. Those techniques and most of the related research works do not consider the interference knowledge exchange between blocks where all the interferences come from, to obtain better performances.

Turbo processing has attracted much attention recently. The technique enhances the reliability of bit information by exchanging the soft information between the detector and the decoder iteratively. One of the techniques that uses the turbo processing concept is the chained turbo equalization (CHATUE) algorithm, proposed by [1]. This paper applies the CHATUE algorithm for the multi user SIMO-OFDM (MU-SIMO-OFDM) systems and provides in-depth convergence property analysis using the extrinsic information transfer (EXIT) chart. It is quite easy to modify the algorithm proposed in this paper such that it can well suited to MIMO-OFDM. This paper also proposes the use of rate-1 doped accumulator for better matching of the EXIT curves of the equalizer and decoder. A series of performance simulations have been

conducted to verify the superiority of the proposed technique.

This paper is organized as follows. The system model used in this paper is presented in Section II. Section III derives the CHATUE algorithm proposed in this paper for MU-SIMO-OFDM without CP. Furthermore, Section III modifies the algorithm with the aim of significantly reducing the complexity. A series of simulations was conducted to evaluate performance of the proposed CHATUE MU-SIMO-OFDM technique. Bit error rate (BER) performance is then presented in Section IV. BER performances are compared between with and without the CHATUE algorithm, as well as with and without doped accumulator. Result of the EXIT chart analysis is used to support the BER simulation results. Finally, Section V concludes this paper.

## II. SYSTEM MODEL

Fig.1 depicts the proposed MU-SIMO-OFDM systems with the CHATUE algorithm. At the transmitter side, each user's stream of information bit sequence  $\mathbf{b}$  are encoded by the encoder  $Enc_c$ , of which results are made statistically independent by using bit interleaver  $\Pi$ , yielding bit-interleaved sequence  $\mathbf{b}_c$ . As in the OFDM system, we use Inverse Fast Fourier Transform (IFFT) to acquire the orthogonality of the signal in order to effectively utilize the spectrum and enhance the robustness over multipath fading. Here  $N$ -point IFFT transforms  $\mathbf{b}_c$  into OFDM symbols with block sequence  $\mathbf{s}$ .

The block  $\mathbf{s}$  is transmitted over frequency-selective quasi-static block Rayleigh fading channel of which the channel matrix has a Toeplitz structure as follows

$$\mathbf{H}_t = \begin{bmatrix} h_0 & & & 0 \\ \vdots & h_0 & & \\ h_{L-1} & \vdots & \ddots & \\ & h_{L-1} & \vdots & h_0 \\ & & \ddots & \vdots \\ 0 & & & h_{L-1} \end{bmatrix}_t \in \mathbb{C}^{(N+L-1) \times N}, \quad (1)$$

where  $L$  is the channel-memory length. Without loss of generality, the channel-memory length is assumed to be equal for all users. Accordingly,  $K_T$  users and  $K_R$  receive antennas in MU-SIMO system create a block-wise channel matrix as

$$\mathbf{H}_t^{i,j} = \begin{bmatrix} \mathbf{H}_t^{1,1} & \mathbf{H}_t^{1,2} & \dots & \mathbf{H}_t^{1,K_T} \\ \mathbf{H}_t^{2,1} & \mathbf{H}_t^{2,2} & \dots & \mathbf{H}_t^{2,K_T} \\ \vdots & \vdots & \ddots & \vdots \\ \mathbf{H}_t^{K_R,1} & \mathbf{H}_t^{K_R,2} & \dots & \mathbf{H}_t^{K_R,K_T} \end{bmatrix}_t \in \mathbb{C}^{(N+L-1)K_R \times NK_T}, \quad (2)$$

$$i = \{1, 2, \dots, K_R\},$$

$$j = \{1, 2, \dots, K_T\}.$$

At the receiver side, we exploit the matrix  $\mathbf{J}$  which was introduced in [7] for non-CP-transmission scheme, to obtain the  $N \times N$  circulant matrix structure of the channel  $\mathbf{H}_c$  as in

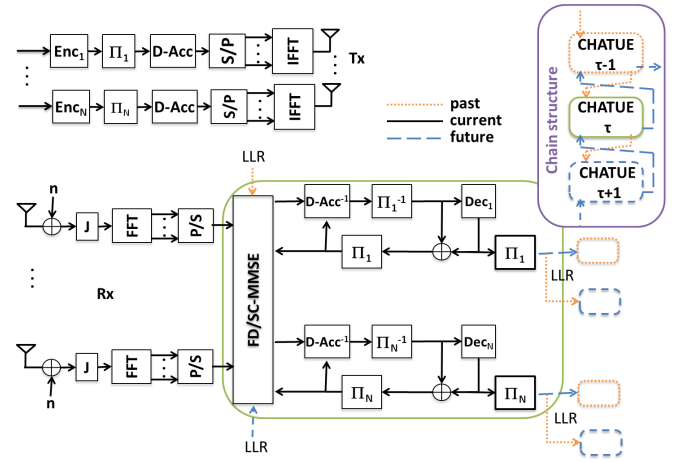


Fig. 1. CHATUE MU-SIMO-OFDM Systems

the CP-transmission schemes. The received signal, suffering from zero mean additive white Gaussian noise (AWGN), can be written as

$$\mathbf{r}_t = \mathbf{J}\mathbf{H}'_{t-1}\mathbf{s}'_{t-1} + \mathbf{J}\mathbf{H}_t\mathbf{s}_t + \mathbf{J}\mathbf{H}''_{t+1}\mathbf{s}''_{t+1} + \mathbf{J}\mathbf{n} \in \mathbb{C}^{NK_T \times 1} \quad (3)$$

after the  $\mathbf{J}$  matrix multiplication, where  $\mathbf{s}'_{t-1}$ ,  $\mathbf{s}_t$ , and  $\mathbf{s}''_{t+1}$  denote  $K_T N \times 1$  vectors of the current, the past, and the future OFDM symbols, respectively. Fast Fourier Transform (FFT) is applied to  $\mathbf{s}$ , in order to retrieve the frequency domain representation of the signal, denoted by  $\mathbf{y}$ .

The use of rate-1 doped-accumulator ( $DAcc$ ) is also considered in this paper. When  $DAcc$  is used at the transmitter, the extrinsic log-likelihood ratio (LLR) obtained by the decoder is fed back to both CHATUE equalizer and de-accumulator, denoted by  $DAcc^{-1}$ . Without  $DAcc^{-1}$ , on the other hand, the extrinsic LLR of the decoder output is provided directly to the equalizer. The input of  $DAcc$  is the coded sequence  $\mathbf{b}_c$ , of which output is referred to as  $\mathbf{x}$ . The purpose of using  $DAcc$  is to achieve better matching of the EXIT curves which will be explained in the Section IV.

In the following, the frequency domain turbo equalizer, FD/SC-MMSE, excellently suppress the channel effect by extracting information about the interference components from the past and the future equalization processes, in the form of LLR. In each time slot, we perform decoding and equalization iteratively. It involves common SIMO FD/SC-MMSE equalizer, de-accumulator, interleaver, de-interleaver, and decoder. In order to provide the *a posteriori* information to the equalizers of the other blocks, coded output of the log-MAP decoder is interleaved and converted to the LLR domain.

## III. CHATUE ALGORITHM FOR MU-SIMO-OFDM

### A. Interferences Cancellation

The equalizer estimates soft symbols of the past block ( $\hat{\mathbf{x}}'_{t-1}$ ), current block ( $\hat{\mathbf{x}}_t$ ), and future block ( $\hat{\mathbf{x}}''_{t+1}$ ) by utilizing

the extrinsic information  $\mathbf{L}_{e,E_{t-1}}$ ,  $\mathbf{L}_{e,E_t}$ , and  $\mathbf{L}_{e,E_{t+1}}$ , respectively, provided by channel decoder of  $K_T$ th user. Note that

$$\hat{\mathbf{x}} = \mathbf{F}\hat{\mathbf{s}} \quad (4)$$

$$\mathbf{F} = \mathbf{I}_{K_R} \otimes \mathbf{F}_N, \quad (5)$$

where  $\mathbf{I}_{K_R}$  is a  $K_R$  identity matrix,  $\mathbf{F}_N$  is an  $N$ -point discrete Fourier Transform matrix, and  $\otimes$  denotes the Kronecker product.  $\hat{\mathbf{x}}'_{t-1}$  and  $\hat{\mathbf{x}}''_{t+1}$  composed of  $K_T$  block(s) are expressed as

$$\hat{\mathbf{x}}'_{t-1} = [\hat{\mathbf{x}}'(1)_{t-1}, \hat{\mathbf{x}}'(2)_{t-1}, \dots, \hat{\mathbf{x}}'(K_T)_{t-1}]^T,$$

$$\hat{\mathbf{x}}'(K_T)_{t-1} = [0, \dots, 0, x_{t-1}^{[N-L+1]}, \dots, x_{t-1}^{[N-1]}] \in \mathbb{C}^{N \times 1}, \quad (6)$$

and

$$\hat{\mathbf{x}}'_{t+1} = [\hat{\mathbf{x}}'(1)_{t+1}, \hat{\mathbf{x}}'(2)_{t+1}, \dots, \hat{\mathbf{x}}'(K_T)_{t+1}]^T,$$

$$\hat{\mathbf{x}}'(K_T)_{t+1} = [x_{t+1}^{[0]}, \dots, x_{t+1}^{[N-1]}, 0, \dots, 0] \in \mathbb{C}^{N \times 1}, \quad (7)$$

respectively. The extrinsic information feedback and its soft bit formation can be written as:

$$L_{e,E_{t-1}} = \ln \frac{\Pr(\hat{b}_{i_{t-1}}) = 0}{\Pr(\hat{b}_{i_{t-1}}) = 1}, \quad x'_{t-1} = \tanh \left[ \frac{L_{e,E_{t-1}}}{2} \right], \quad (8)$$

$$L_{e,E_t} = \ln \frac{\Pr(\hat{b}_{i_t}) = 0}{\Pr(\hat{b}_{i_t}) = 1}, \quad x_t = \tanh \left[ \frac{L_{e,E_t}}{2} \right], \quad (9)$$

$$L_{e,E_{t+1}} = \ln \frac{\Pr(\hat{b}_{i_{t+1}}) = 0}{\Pr(\hat{b}_{i_{t+1}}) = 1}, \quad x''_{t+1} = \tanh \left[ \frac{L_{e,E_{t+1}}}{2} \right], \quad (10)$$

where  $\hat{\mathbf{b}}_t = \Pi\{\hat{\mathbf{b}}_c\}$  with  $\Pi\{\bullet\}$  being the interleaving function. These soft symbols are used to form three soft replicas,  $\mathbf{F}\mathbf{J}\mathbf{H}_t\mathbf{F}^H\hat{\mathbf{x}}_t$ ,  $\mathbf{F}\mathbf{J}\mathbf{H}'_{t-1}\mathbf{F}^H\hat{\mathbf{x}}'_{t-1}$  and  $\mathbf{F}\mathbf{J}\mathbf{H}''_{t+1}\mathbf{F}^H\hat{\mathbf{x}}''_{t+1}$ . Soft replica  $\mathbf{F}\mathbf{J}\mathbf{H}_t\mathbf{F}^H\hat{\mathbf{x}}_t$  is used for the ICI cancellation within the  $t$ -block, whereas  $\mathbf{F}\mathbf{J}\mathbf{H}'_{t-1}\mathbf{F}^H\hat{\mathbf{x}}'_{t-1}$  and  $\mathbf{F}\mathbf{J}\mathbf{H}''_{t+1}\mathbf{F}^H\hat{\mathbf{x}}''_{t+1}$  are used for the ISI cancellation as well as MAI cancellation, from the past and future blocks, respectively. Furthermore, soft cancellation to the received signal is performed by using these soft replicas. The residual of the soft cancellation can be expressed

$$\tilde{\mathbf{y}}_t = \mathbf{F}\mathbf{J}\mathbf{H}'_{t-1}\mathbf{F}^H(\mathbf{x}'_{t-1} - \hat{\mathbf{x}}'_{t-1}) + \mathbf{F}\mathbf{J}\mathbf{H}_t\mathbf{F}^H(\mathbf{x}_t - \hat{\mathbf{x}}_t) + \mathbf{F}\mathbf{J}\mathbf{H}''_{t+1}\mathbf{F}^H(\mathbf{x}''_{t+1} - \hat{\mathbf{x}}''_{t+1}) + \mathbf{F}\mathbf{J}\mathbf{n}. \quad (11)$$

We also use  $\Phi\hat{\mathbf{x}}_t = \mathbf{F}\mathbf{J}\mathbf{H}_t\mathbf{F}^H\hat{\mathbf{x}}_t$  as a restoral term, i.e. the main signal when all the interferences are totally cancelled.

### B. MMSE Filter

The remaining part of the algorithm is to suppress the residual left after the soft cancellation. We use linear filtering with objective of minimizing the mean square error between the filter output and the signal, for which criterion is given by

$$\mathbf{W} = \arg \min_{\mathbf{W}} E \left\{ \left\| \hat{\mathbf{x}}_t - \mathbf{W}^H \tilde{\mathbf{y}}_t \right\|^2 \right\}, \quad (12)$$

where  $\bar{\mathbf{y}} = \tilde{\mathbf{y}}_t + \Phi\hat{\mathbf{x}}_t$ . Derivation of optimum matrix  $\mathbf{W}$  leads to the weight vector of MMSE filtering, as:

$$\mathbf{W}^H = \left( \mathbf{1}_{NK_T \times NK_R} + \Gamma \hat{\mathbf{X}}_t \right)^{-1} \Phi^H \Sigma^{-1}, \quad (13)$$

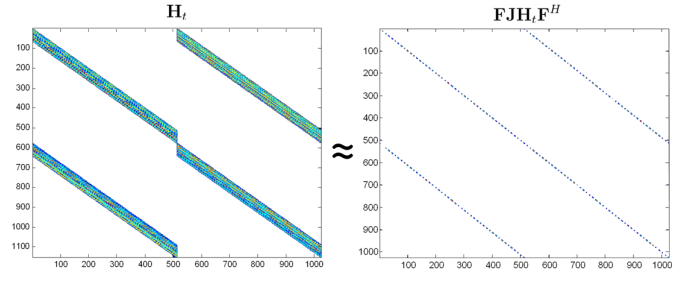


Fig. 2. Diagonal structure of matrix  $\mathbf{F}\mathbf{J}\mathbf{H}_t\mathbf{F}^H$

where  $\mathbf{1}_{NK_T \times NK_R}$  is all one  $NK_T \times NK_R$  matrix,  $\hat{\mathbf{X}}_t$  is a covariance matrix of  $\hat{\mathbf{x}}_t$ ,  $\Gamma = \Phi^H \Sigma^{-1} \Phi$ , and  $\Sigma$  is given by

$$\begin{aligned} \Sigma &= \mathbf{F}\mathbf{J}\mathbf{H}'_{t-1}\mathbf{F}^H \Lambda'_{t-1} (\mathbf{F}\mathbf{J}\mathbf{H}'_{t-1}\mathbf{F}^H)^H + \Phi \Lambda_t (\Phi)^H \\ &\quad + \mathbf{F}\mathbf{J}\mathbf{H}''_{t+1}\mathbf{F}^H \Lambda''_{t+1} (\mathbf{F}\mathbf{J}\mathbf{H}''_{t+1}\mathbf{F}^H)^H + \mathbf{F}\sigma^2 \mathbf{J}\mathbf{J}^H \mathbf{F}^H, \\ \Phi &= \mathbf{F}\mathbf{J}\mathbf{H}_t\mathbf{F}^H. \end{aligned} \quad (14)$$

$\Lambda'_{t-1}$ ,  $\Lambda_t$ , and  $\Lambda''_{t+1}$  are  $NK_T \times NK_R$  covariance matrices of the interference components.  $\sigma^2$  denotes the noise variance.

Finally, the equalizer output can be obtained as

$$\begin{aligned} \mathbf{z} &= \mathbf{W}^H \bar{\mathbf{y}} \\ &= \left( \mathbf{1}_{NK_T \times NK_R} + \Gamma \hat{\mathbf{X}} \right)^{-1} (\Phi^H \Sigma^{-1} \bar{\mathbf{y}} + \Gamma \hat{\mathbf{x}}). \end{aligned} \quad (15)$$

In the following, some approximations of  $\Sigma^{-1}$  are considered to reduce the computational complexity.

### C. Complexity Reduction

The computational complexity of (15) is due mostly to the inversion of matrix  $\Sigma^{-1}$ . Consider the equation (14),  $\Sigma$  comprises of three major matrices, as follows

$$\begin{aligned} \mathbf{A} &= \Phi \Lambda_t (\Phi)^H \\ \mathbf{B} &= \mathbf{F}\mathbf{J}\mathbf{H}'_{t-1}\mathbf{F}^H \Lambda'_{t-1} (\mathbf{F}\mathbf{J}\mathbf{H}'_{t-1}\mathbf{F}^H)^H \\ &\quad + \mathbf{F}\mathbf{J}\mathbf{H}''_{t+1}\mathbf{F}^H \Lambda''_{t+1} (\mathbf{F}\mathbf{J}\mathbf{H}''_{t+1}\mathbf{F}^H)^H \\ \mathbf{C} &= \mathbf{F}\sigma^2 \mathbf{J}\mathbf{J}^H \mathbf{F}^H. \end{aligned} \quad (16)$$

Matrix  $\mathbf{A}$  contains diagonal submatrices which was originally formed by the Toeplitz structure of submatrices of  $\mathbf{H}_t$  with density shown in Fig. 2. Matrix  $\mathbf{J}$  makes the matrix  $\mathbf{H}_t$  circulant. Recall that a circulant channel matrix in the time domain can be converted into a diagonal matrix in the frequency domain also as shown in Fig. 2. Since  $\Lambda_t$  can be approximated by diagonal matrix, eventually we have a similar circulant structure of matrix  $\mathbf{A}$ .

Furthermore, let the matrix  $\mathbf{B}$  be divided into submatrices  $\mathbf{B}_{ij}$  with  $i = \{1, 2, \dots, K_R\}$  and  $j = \{1, 2, \dots, K_T\}$ . Without loss of generality, Fig. 3 shows the density of those submatrices for  $K_R = K_T = 2$ . Each submatrix has density only at the top-left and bottom-right corners of the matrix. We apply approximation by taking only the diagonal part of those *matrix corners*, yielding  $\mathbf{B}'_{ij}$ . Since  $\mathbf{B}'_{ij}$  is a diagonal elements, it is also reasonable to use the approximation as follows:

$$\mathbf{F}_N \mathbf{B}'_{ij} \mathbf{F}_N^H = \frac{1}{N} \text{tr}(\mathbf{B}'_{ij}) \mathbf{I}_N, \quad (17)$$

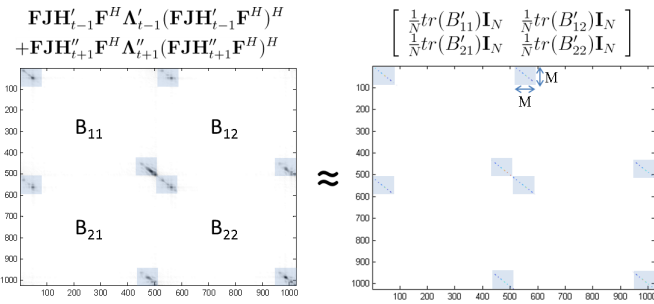


Fig. 3. Approximations of matrix  $\mathbf{B}$  at *a priori* mutual information of past and future = 0.5

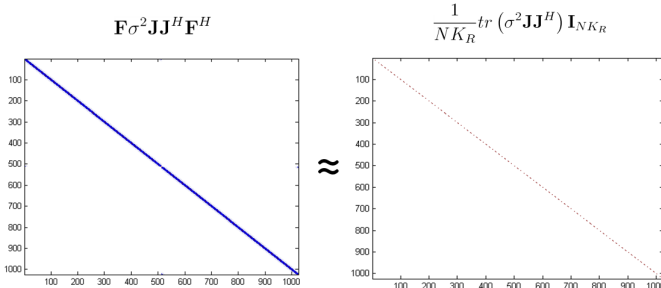


Fig. 4. Approximations of matrix  $\mathbf{C}$  at *a priori* mutual information of past and future = 0.5

where  $\text{tr}\{\bullet\}$  is the trace of its argument matrix  $\bullet$ .

Finally, in the same way as the approximation used for the matrix  $\mathbf{B}$ , the matrix  $\mathbf{C}$  can be approximated as

$$\mathbf{F}\sigma^2\mathbf{J}\mathbf{J}^H\mathbf{F}^H \approx \frac{1}{NK_R}\text{tr}[\sigma^2\mathbf{J}\mathbf{J}^H]\mathbf{I}_{NK_R}, \quad (18)$$

as shown in Fig. 4.

Now we have  $\Sigma$  with only diagonal submatrices. Hence,  $\Sigma^{-1}$  can easily be calculated.

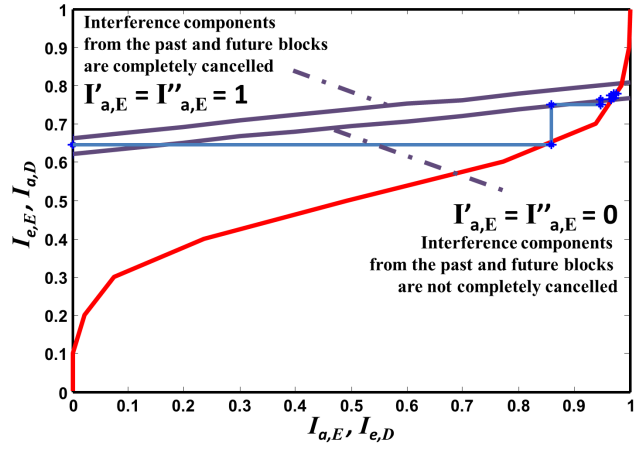
#### IV. SIMULATION RESULTS

##### A. EXIT Chart Analysis

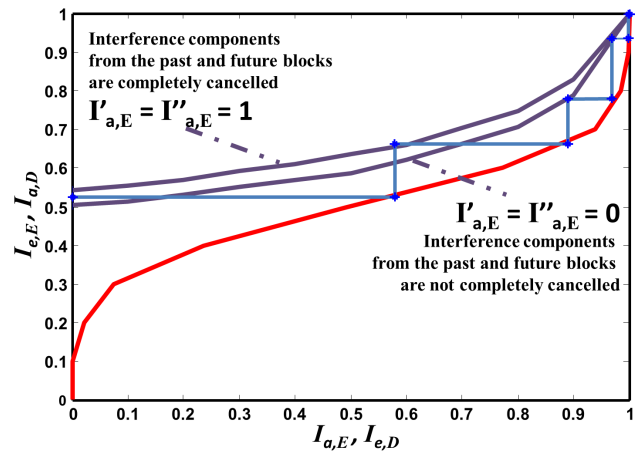
Fig. 5 shows the EXIT curves of the equalizer and the decoder for  $E_b/N_o = 5$  dB. Note that  $E_b/N_o = \text{SNR} \times \frac{1}{R}$ , with  $R$

TABLE I  
SIMULATION PARAMETERS

Transmitter	Antenna Modulation DFT/IDFT size Encoder Interleaver doping ratio CP ratio	$K_T = 2, K_R = 2$ BPSK 512 NSNRCC with GP = [5,7] Random 4 1/8
Channel	Multipath Selective Fading Multipath Selective Fading	rural area (COST 207) bad urban (COST 207)
Receiver	Equalizer Iterations Channel Estimation Synchronization Decoder	FD/SC-MMSE 4 Perfect Perfect log-MAP BCJR



(a)



(b)

Fig. 5. EXIT analysis of two extreme cases of CHATUE-MU-SIMO-OFDM without (a) and with accumulator (b) at  $E_b/N_o = 5$  dB

being the channel coding rate. A half-rate non-systematic non-recursive convolutional coding (NSNRCC) with the constraint length equal to three and a generator polynomial  $G = [7, 5]$  is considered. The trajectory of the mutual information exchange is also shown in Fig. 5. For the simplicity, we only plot the lower and upper bound EXIT curves. The lower bound is obtained by setting  $I'_{a,E} = I''_{a,E} = 0$ , which corresponds to the case where all ISI components remains. Whereas the upper bound is obtained by setting  $I'_{a,E} = I''_{a,E} = 1$ , which corresponds to the case where all ISI components are completely cancelled. The EXIT curve of the decoder is drawn by measuring the histogram of the decoder output LLR.

A decoding trajectory visualizes the exchange of extrinsic information between constituent soft-input-soft-output (SISO) blocks, which are the equalizer and the channel decoder. A simulation for generating the trajectory line is organized as the following. Three consecutive equalizer blocks are connected in time, i.e.  $EQ_{t-1}$ ,  $EQ_t$ ,  $EQ_{t+1}$  as the past, the present, and the future blocks, respectively. The past feedback mutual

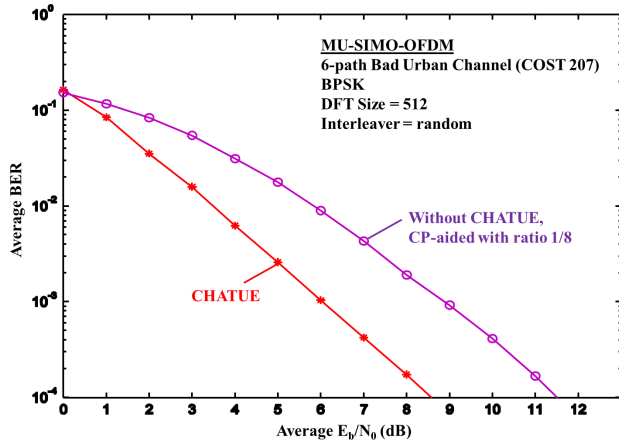


Fig. 6. BER performance of MU-SIMO-OFDM, with and without CHATUE comparison

information of the past block, as well as the future feedback mutual information of the future block are set at zero. We start evaluated the mutual information between the input of channel decoder and the coded bits  $\mathbf{b}_c$  of the present block, denotes by  $I_{e,E} = I_{a,D}$ , iteration-by-iteration. Here the extrinsic mutual information from the decoder to the  $EQ_t$ , denotes by  $I_{e,D} = I_{a,E}$ , is set at zero as the initial value, afterwards, the step-wise line are drawn by evaluating  $I_{e,E}$  and  $I_{a,E}$ , according to the iterations. Fig. 5 illustrates that no more significant iteration gain is obtained after four iterations.

Fig. 5(a) shows the EXIT chart without using *DAcc* in the systems. It is found that with the mutual information feedback from the past and the future being zero, the EXIT curves intersect each other, which makes the trajectory can not reach the  $I_{e,D} = 1$ . With the mutual information from the past and the future block being one, the EXIT curves intersect each other as well. Therefore, we can not reduce the error probability to arbitrarily small.

To avoid this problem, a modification was introduced by exploiting *DAcc* and adjusting the doping rate  $P$  in *DAcc* to adjust the equalizer EXIT curve so that the convergence tunnel opens up to the (1,1) mutual information point, as shown in the Fig. 5(b). This paper use  $P = 4$  as the doping rate. It is found that a point close enough to the (1,1) mutual information point can be reached without having intersection. Furthermore, in the range of  $I_{a,E} \geq 0.3$ , the two EXIT curves have a similar shape. Therefore, we can expect to achieve a clear turbo cliff in static frequency-selective channels. However, this paper more focus on average performance in fading channels, thereby average BER versus average  $E_b/N_0$  will be provided in the next subsection.

### B. Performance Evaluation

Computer simulations were conducted to evaluate the performances, using the parameters shown in table I. All random interleaver length are 512 in bits. For fair comparison, the coding rate was adjusted while keeping the number of the

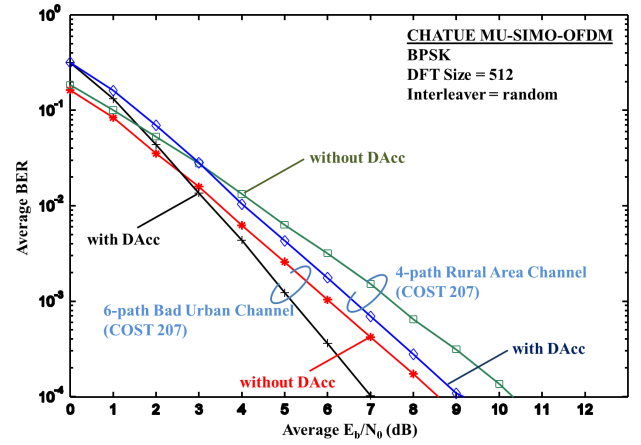


Fig. 7. BER performance of MU-SIMO-OFDM

information bits in one block (including the CP length in the case of CP-transmission) constant for the both proposed and the conventional CP-transmission cases.

We use multipath selective fading channel based on COST 207 channel models [6]. Here we select rural-area and bad-urban channel models as representative of wide range application to the channel conditions. We use bad-urban channel model for the performance comparison between CP-aided and non-CP-aided transmission scheme. We also assume that the receiver has perfect knowledge about the channel.

Fig. 6 shows roughly 3 dB gain in  $E_b/N_0$  can be achieved with non-CP-aided transmission at  $BER = 10^{-4}$  over the CP-aided transmission scheme. Obviously, the gain is due to the utilization of the strong code (lower rate), made possible by eliminating the CP. The performances of CHATUE in bad-urban and rural-area channel models are shown in Fig. 7. In general, the more the multipath, the higher the diversity gain, and thereby the CHATUE performance improvement is decreased in rural-areas. However, still in average, about 1.3 dB improvement can be achieved at  $BER = 10^{-4}$  by utilizing *DAcc*. These results confirm the analysis that has been shown in the EXIT Chart analysis subsection.

### V. CONCLUSION

The CHATUE algorithm has been applied to MU-SIMO-OFDM systems with the aim of avoiding the loss in spectral efficiency and suppressing the ISI, ICI, and MAI components. To avoid computationally heavy matrix inversion, several approximation techniques are introduced when deriving the proposed algorithm. It can be concluded that the proposed systems can remove the loss in spectral efficiency due to the use of CP, while significantly improving the performances compared to the conventional CP-aided MU-SIMO-OFDM systems. The computational complexity with the proposed systems is as small as the conventional CP-aided transmission, because the proposed systems also utilizes the advantageous points of the frequency domain processing, together with some proposed mathematical approximations.

## REFERENCES

- [1] Anwar, K., Zhou, H., Matsumoto, T.: Chained turbo equalization for block transmission without guard interval. In: IEEE VTC2010-Spring. Taiwan (2010)
- [2] boroujeny B., F., S., G.: Generalized sliding fft and its application to implementation of block lms adaptive filters. *IEEE Trans. Signal Processing* **42**, 532–538 (1994)
- [3] Beheshti, M., Omid, M., Doost-Hoseini, A.: Equalisation of simo-ofdm systems with insufficient cyclic prefix in doubly selective channels. *IET Communications* **3**, 1870–1882 (2009)
- [4] Chen, Z., Yongyu, C., Yang, D.: Low-complexity turbo equalization for MIMO-OFDM system without cyclic prefix. In: IEEE PIMRC 2009. Tokyo (2009)
- [5] Lim, J.B., Choi, C.H., Im, G.H.: MIMO-OFDM with insufficient cyclic prefix. In: *IEEE Communications Letter*, vol. 10, pp. 356–358 (2006)
- [6] Patzold, M.: *Mobile Fading Channel*, p. 259. John Wiley & Sons (2002)
- [7] Wang, D., Wei, C., Pan, Z., You, X., Kyuu, C.H., Jang, J.B.: Low-complexity turbo equalization for single-carrier systems without cyclic prefix. In: *IEEE ICC*, pp. 1091–1095. Beijing (2008)
- [8] Y.S., C., P.J., V., F.A., C.: On channel estimation and detection for multicarrier signals in fast and selective rayleigh fading channels. *IEEE Trans. Communication* **49**, 1375–1387 (2001)
- [9] Yu, J.L., Lee, M.C., Chen, C.H.: Finite sample performance of channel estimation and equalization for simo ofdm systems without cyclic prefix. In: *TENCON 2007 - IEEE Region 10 Conference*, pp. 1–4. Taipei (2007)